Simulation of Swimming Organisms: Coupling Internal Mechanics with External Fluid Dynamics

Problems in biological fluid dynamics typically involve the interaction of an elastic structure with its surrounding fluid. A unified computational approach, based on an immersed boundary framework, couples the internal force-generating mechanisms of organisms and cells with an external, viscous, incompressible fluid.

Computational simulation, in conjunction with laboratory experiment, can provide valuable insight into complex biological systems that involve the interaction of an elastic structure with a viscous, incompressible fluid. This biological fluid dynamics setting presents several more challenges than those traditionally faced in computational fluid dynamics—specifically, dynamic flow situations dominate, and capturing time-dependent geometries with large structural deformations is necessary. In addition, the shape of the elastic structures is not preset: fluid dynamics determines it.

The Reynolds number of a flow is a dimensionless parameter that measures the relative significance of inertial forces to viscous forces. Due to the small length scales, the swimming of microorganisms cor-

responds to very small Reynolds numbers (10^{-6} – 10^{-2}). Faster and larger organisms such as fish and eels swim at high Reynolds numbers (10^2 – 10^5), but organisms such as nematodes and tadpoles experience inertial forces comparable to viscous forces: they swim at Reynolds numbers of order one.

Modern methods in computational fluid dynamics can help create a controlled environment in which we can measure and visualize the fluid dynamics of swimming organisms. Accordingly, we designed a unified computational approach, based on an immersed boundary framework,[1] that couples internal force-generation mechanisms of organisms and cells with an external, viscous, incompressible fluid. This approach can be applied to model low, moderate, and high Reynolds number flow regimes.

Analyzing the fluid dynamics of a flexible, swimming organism is very difficult, even when the organism's waveform is assumed in advance.[2,3] In the case of microorganism motility, the low Reynolds number simplifies mathematical analysis because the equations of fluid mechanics in this regime are linear. However, even at low Reynolds numbers, a microorganism's waveform is an emergent property of the coupled nonlinear system, which consists of the organism's force-generation mechanisms, its passive elastic structure, and external fluid dynamics. In the immersed boundary framework, the force-generat-

Ricardo Cortez and Lisa Fauci
Tulane University
Nathaniel Cowen
Courant Institute of Mathematical Sciences
Robert Dillon
Washington State University

ing organism is accounted for by suitable contributions to a force term in the fluid-dynamics equations. The force of an organism on the fluid is a Dirac delta-function layer of force supported only by the region of fluid that coincides with the organism's material points; away from these points, this force is zero. After including this force distribution on the fluid, we can solve the fluid equations by using either a finite-difference grid-based method or the *regularized Stokeslets* grid-free method developed specifically for zero Reynolds number regimes.[4]

This article presents our recent progress on coupling the internal molecular motor mechanisms of beating cilia and flagella with an external fluid, as well as the three-dimensional (3D) undulatory swimming of nematodes and leeches. We expect these computational models to provide a testbed for examining different theories of internal force-generation mechanisms.

Immersed Boundary Framework

Charles Peskin[1] introduced the immersed boundary method to model blood flow in the heart. Since then, many researchers have advanced this method to study other biologic fluid dynamics problems, including platelet aggregation, 3D blood flow in the heart, inner-ear dynamics, blood flow in the kidneys, limb development, and deformation of red blood cells; a recent overview appears elsewhere.[1]

For this article's purposes, we describe the immersed boundary method in the context of swimming organisms. We regard the fluid as viscous and incompressible, and the filaments that comprise the organisms as elastic boundaries immersed in this fluid. In our 3D simulations—Figure 1 shows a typical example—many filaments join to form the organism. The nematode, tapered at both ends, is built out of three families of filaments: circular, longitudinal, and right- and left-handed helical filaments.

We assume that the flow is governed by the incompressible Navier-Stokes equations (conservation of momentum and conservation of mass):

$$\rho\left[\frac{\partial \mathbf{u}}{\partial t} + \mathbf{u} \cdot \nabla\mathbf{u}\right] = -\nabla p + \mu\nabla\mathbf{u} + \mathbf{F}(\mathbf{x}, t)$$

$$\mathbf{F} = \sum_k \mathbf{F}^k$$

$$\nabla \cdot \mathbf{u} = 0.$$

Here, ρ is fluid density, μ is dynamic viscosity, $\mathbf{u}$ is fluid velocity, p denotes pressure, and $\mathbf{F}$ is the force per unit volume the organism exerts on the fluid—this force is split into the contributions from each of the filaments comprising the organism. The forces $\mathbf{F^k}$ due to the kth filament include elastic

(a) **(b)**
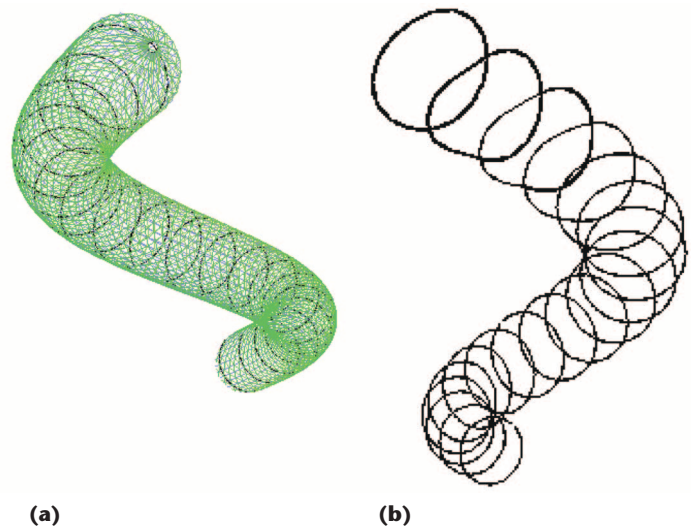
Figure 1. Three-dimensional nematode. (a) An immersed boundary nematode, and (b) a snapshot of a swimming nematode suppressing all but the "circular" filaments. Notice that these filaments are elastic and deform in response to the viscous fluid.

forces from individual filament structures and passive elastic forces caused by links between filaments; they also may include active forces due to muscle contractions (in the case of nematode or leech swimming) or active forces caused by the action of dynein molecular motors (in the case of ciliary and flagellar beating). $\mathbf{F}$ is a δ-function layer of force supported only by the region of fluid that coincides with the filaments' material points; away from these points, the force is zero.

Let $\mathbf{X}^k(s, t)$ denote the kth filament as a function of a Lagrangian parameter s and time t, and let $\mathbf{f}^k(s, t)$ denote the boundary force per unit length along the kth filament. The boundary force depends on the biological system being modeled; we'll discuss the general form later. We assume the elastic boundary has the same density as the surrounding fluid, and that its mass is attributed to the mass of the fluid in which it sits, thus the forces are transmitted directly to the fluid. The force field $\mathbf{F}^k$ from the filament $\mathbf{X}^k(s, t)$ is therefore

$$\mathbf{F}^k(\mathbf{x}, t) = \int \mathbf{f}^k(s, t)\, \delta\,(\mathbf{x} - \mathbf{X}^k(s, t))ds.$$

Here, the integration is over the kth one-dimensional filament comprising an immersed boundary, and δ is the 3D Dirac delta-function. The total force $\mathbf{F}(\mathbf{x}, t)$ is calculated by adding the forces from each filament.

Each filament of the immersed boundary is approximated by a discrete collection of points. This boundary exerts elastic forces on the fluid near each of these points. We imagine that between each pair
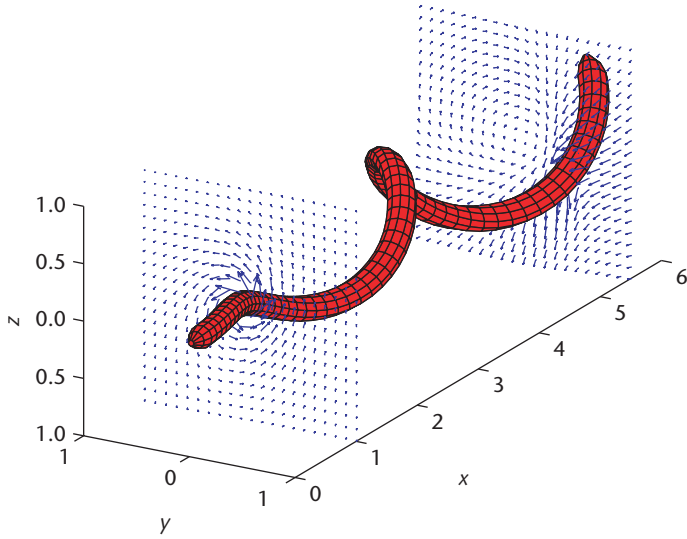
Figure 2. A bacterium swimming because of a helical wave's propagation. Fluid velocity vectors are shown on two planes perpendicular to the swimming axis. The simulation demonstrates the grid-free method of regularized Stokeslets.

of successive points on a filament, an elastic spring or *link* generates forces to push the link's length toward a specified resting length. The force arising from the spring on a short filament segment of length *ds* is the product of a stiffness constant and the deviation from rest length. This force is approximated by the force density at a single point in the segment multiplied by *ds*. In addition to the forces caused by springs along individual filaments, forces due to passive or active interactions between filaments contribute to force density. Each spring may have a time-dependent rest length as well as a time-dependent stiffness. Our coupled fluid-immersed boundary system is closed because it requires the velocity of a filament's material point to be equal to the fluid velocity evaluated at that point.

In the next two sections, we provide brief descriptions of two numerical methods used in the simulation of immersed boundary motion in flows corresponding to a wide range of Reynolds numbers.

Grid-Based Immersed Boundary Algorithm

We can summarize the immersed boundary algorithm as follows: Suppose that at the end of time step n, we have fluid velocity field $\mathbf{u}^n$ on a grid and the configuration of the immersed boundary points on the filaments comprising the organism $(\mathbf{X^k})^n$. To advance the system by one time step, we must

1. Calculate the force densities $\mathbf{f^k}$ from the boundary configuration.
2. Spread the force densities to the grid to determine the forces $\mathbf{F^k}$ on the fluid.
3. Solve the Navier-Stokes equations for $\mathbf{u}^{n+1}$.
4. Interpolate the fluid velocity field to each immersed boundary point $(\mathbf{X^k})^n$ and move the point at this local fluid velocity.

The Navier-Stokes equations are solved on a regular grid with simple boundary conditions in Step 3; Steps 2 and 4 involve the use of a discrete delta-function that communicates information between the grid and the immersed boundary points.[1] This algorithm's crucial feature is that the immersed boundary is not the computational boundary in the Navier-Stokes solver—rather, it is a dynamic force field that influences fluid motion via the force term in the fluid equations. This modular approach lets us choose a fluid solver best suited to the problem's Reynolds number. Furthermore, we can base whatever solver we choose on a variety of formulations, including finite-difference and finite-element methods.

Grid-Free Method of Regularized Stokeslets

At the low Reynolds number regime of swimming microorganisms, we can describe the fluid dynamics via the quasi-steady Stokes equations:

$$\mu\Delta\mathbf{u} = \nabla p - \mathbf{F}(\mathbf{x}, t)$$
$$\nabla \cdot \mathbf{u} = 0.$$

A fundamental solution of these equations is called a Stokeslet, which represents the velocity due to a concentrated force acting on the fluid at a single point in an infinite domain of fluid.[3] In fact, $\mathbf{F}(\mathbf{x}, t)$ is the sum of such point forces. Ricardo Cortez considered the smoothed case in which the concentrated force is applied not at a single point, but over a small ball of radius ε centered at the immersed boundary point.[4] We can compute a regularized fundamental solution—or regularized Stokeslet—analytically. The method of regularized Stokeslets is a Lagrangian method in which the trajectories of fluid particles are tracked throughout the simulation. This method is particularly useful when the forces driving the fluid motion are placed along the surface of a swimming organism that deforms because of its interaction with the fluid. The forces on the surface are given by regularized delta-functions, and the resulting velocity represents the exact solution of Stokes equations for the given forces.

Because the incompressible Stokes equations are linear, we can use direct summation to compute the velocity at each immersed boundary point to advance a time step. This method of regularized

Stokeslets is related to boundary integral methods, but it has the advantage that forces may be applied at any discrete collection of points—these points need not approximate a smooth interface.

We have successfully implemented this algorithm for ciliary beating in two dimensions and helical swimming in three. Figure 2 shows a snapshot of a helical swimmer with fluid velocity fields computed along two planes perpendicular to the axis of the helix.

Undulatory Swimming

Nematodes are unsegmented roundworms with elongated bodies tapered at both ends. The most famous nematode is *C. Elegans*, a model organism for genetic, developmental, and neurobiological studies. Nematodes possess a fluid-filled cavity, longitudinal muscles, and a flexible outer cuticle composed of left- and right-handed helical filaments, yet they still maintain a circular cross-section. The alternate contractions of their dorsal and ventral longitudinal muscles cause these worms to swim with an eel-like, undulatory pattern.[5] A typical nematode is roughly 0.5 to 1 millimeter long, undulating with a wave speed between 0.8 and 4 millimeters per second. Therefore, in water, a Reynolds number (based on wavelength and wave speed) between 0.4 and 4 governs nematode swimming.

We chose the filaments comprising our computational organism to reflect the nematode's anatomy, including the longitudinal muscle fibers and the helical filaments of its cuticle. The stiffness constants of the "springs" making up these filaments reflect the tissue's elastic properties. In the simulation depicted in Figure 1, sinusoidal undulatory waves are passed along the body of the immersed organism by imposing appropriate muscle contractions along its longitudinal and helical filaments. Figure 3 shows a 3D perspective of the worm along with the velocity field of the fluid depicted in the plane that contains the worm's centerline. (Here, we used a grid-based immersed boundary algorithm.) The flow field shows vortices with alternating directions supported along the length of the organism. A previous study experimentally observed this characteristic flow pattern for the nematode *Turbatrix*.[5] We computed the swimming speed of our simulated nematode, whose amplitude of oscillation we chose to be about one half of that reported for *Turbatrix*, to be 5 percent of the propulsive wave speed along its body. These calculations compare very well with the experimentally observed swimming speed of 20 percent of wave speed reported for *Turbatrix*;[5] swimming speed is proportional to the square of the wave's amplitude.[2]

We now turn to modeling another undulatory
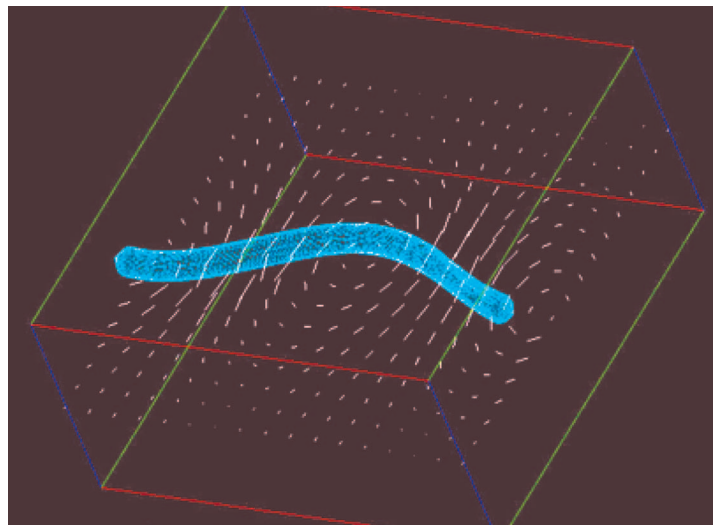
Figure 3. Snapshot of a swimming nematode shown within the rectangular computational domain. The velocity field is depicted in the plane that contains the worm's centerline.

swimmer—the leech. Leeches are larger and faster than nematodes, and have an elliptical rather than circular cross-section. We focus on 2-centimeter long juvenile leeches, with propulsive wave speeds of approximately 5 centimeters per second undulating in water. In this case, the Reynolds number based on wavelength and wave speed is about 1,000; inertial effects are significantly more important than viscous effects.[6]

Using the same immersed boundary construct as we did for the nematodes (longitudinal muscle filaments and right- and left-helical filaments), but replacing the circular filaments with elliptical cross-sectional filaments, we examine the leech's undulatory swimming in a 3D fluid. Figure 4 shows four snapshots of the leech as viewed from the side, along with fluid markers for flow visualization. Each of the four snapshots depicts the leech at the same phase in its undulation, during successive periods. A wave passes over the body from left to right—note the forward swimming progression and the wake that is left behind. We initially placed the red fluid markers in the foreground far enough from the side of the leech that they don't get carried along with the organism. Figure 5 shows four snapshots of the leech from a different perspective—note the complex 3D particle mixing that occurs.

For our simulated leech, we used experimental data on waveform and wave speed originally reported by Chris Jordan.[6] Because of accuracy constraints that require enough grid points within a cross-section of the leech, the aspect ratio of the simulated leech's elliptical cross-section is 2:1, not
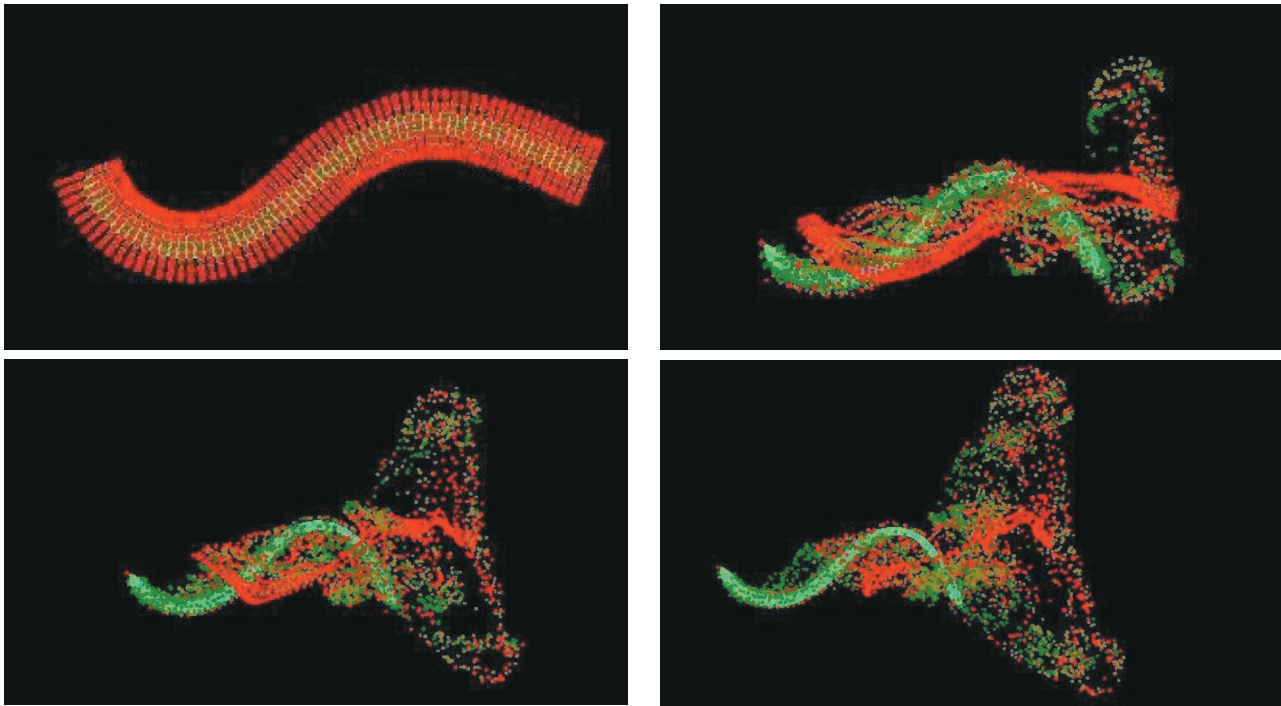
Figure 4. Snapshots of leech and surrounding fluid markers at the same phase in its undulation during successive temporal periods. The actual organism is mostly obscured in the first panel by the fluid markers placed around it.

the actual 5:1 Jordan reported.[6] We believe that this difference causes the simulated leech to swim about five times slower than the real leech.

Cilia and Flagella

Cilia and flagella are the prominent organelles associated with microorganism motility. Although the patterns of flagellar movement are distinct from those of ciliary movement, and flagella are typically much longer than cilia, their basic ultrastructure is identical. A core—called the *axoneme*—produces the bending of cilia and flagella. The typical axoneme consists of a central pair of single microtubules surrounded by nine outer doublet microtubules and encased by the cell membrane.[7,8] Radial spokes attach to the peripheral doublet microtubules and span the space toward the central pair of microtubules. The outer doublets are connected by nexin links between adjacent pairs of doublets. Two rows of dynein arms extend from the A-tubule of an outer doublet toward the B-tubule of an adjacent doublet at regularly spaced intervals. The bending of the axoneme is caused by sliding between pairs of outer doublets, which in turn is due to the unidirectional adenosine triphosphate (ATP)-induced force generation of the dynein molecular motors. The precise nature of the spatial and temporal control mechanisms regulating the various waveforms of cilia and flagella is still unknown.

Considerable interest has focused on the development of mathematical models for the hydrodynamics of individual as well as rows of cilia and on individual flagellated organisms. Gray and Hancock's[9] resistive-force theory and Sir James Lighthill's slender body theory[3] are particularly noteworthy. More detailed hydrodynamic analysis, such as refined slender body theory and boundary element methods, have produced excellent simulations of both two- and three-dimensional flagellar propulsion and ciliary beating in an infinite fluid domain or in a domain with a fixed wall. In all these fluid dynamical models, researchers take the shape of the ciliary or flagellar beat as given. More recent work by Shay Gueron and Konstantin Levit-Gurevich includes a model that addresses the internal force generation in a cilium[10] but does not explicitly model the individual microtubule-dynein interactions.

Our model for an individual cilium or flagellum incorporates discrete representations of the dynein arms, passive elastic structures of the axoneme including the microtubules and nexin links, and the surrounding fluid. This model couples the internal force generation of the molecular motors through the passive elastic structure with external fluid mechanics. Detailed geometric information may be kept track of in this computational model, such as the spacing and shear between the microtubules, the local curvature of individual microtubules, and the
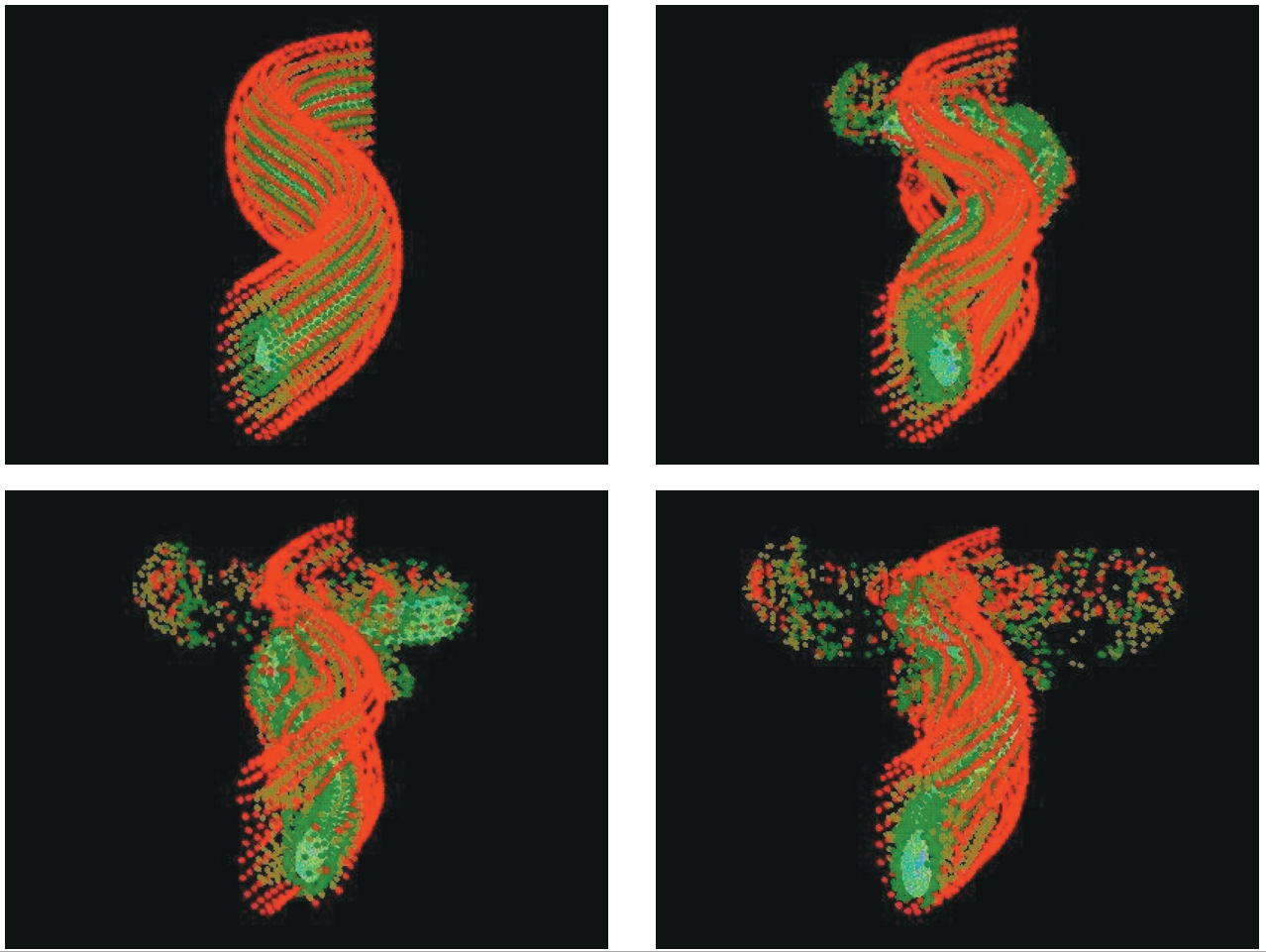
Figure 5. Snapshots of leech and surrounding fluid markers. From this perspective, the wave is moving back over the body, and the swimming progression is toward the viewer. Note the complex 3D fluid mixing depicted by the evolution of the fluid markers.

stretching of the nexin links. In addition, the explicit representation of the dynein motors gives us the flexibility to incorporate a variety of activation theories. The ciliary beat or flagellar waveform is not preset, but it is an emergent property of the interacting components of the coupled fluid-axoneme system.

In other articles,[11,12] we present a model of a simplified axoneme consisting of two microtubules, with dynein motors being dynamic, diagonal elastic links between the two microtubules. To achieve beating in the simplified two-microtubule model, we allow two sets of dyneins to act between the microtubules—one set is permanently attached to fixed nodes on the left microtubule, the other to fixed nodes on the right. Contraction of the dynein generates sliding between the two microtubules; in either configuration, one end of a dynein can attach, detach, and reattach to attachment sites on the microtubule. As the microtubules slide, a dynein link's endpoint can jump, or "ratchet," from

one node of the microtubule to another.

We model each microtubule as a pair of filaments with diagonal cross-links. The diagonal cross-links' elastic properties govern the resistance to microtubule bending. Linear elastic springs representing the nexin and/or radial links of the axoneme interconnect adjacent pairs of microtubules. In the case of ciliary beating, the axoneme is tethered to fixed points in space via strong elastic springs at the base. The entire structure is embedded in a viscous incompressible fluid.

Figure 6 shows a cilium during the power stroke (note the two microtubules) and a ciliary waveform showing a single filament at equally spaced time intervals. This waveform was not preset—it resulted from the actions of individual dynein motors. In particular, the cilium's local curvature determined the activation cycle of each dynein motor along the cilium. Figure 7 shows the swimming of a model sperm cell whose waveform is also the result of a curvature con-

(a)

(b)
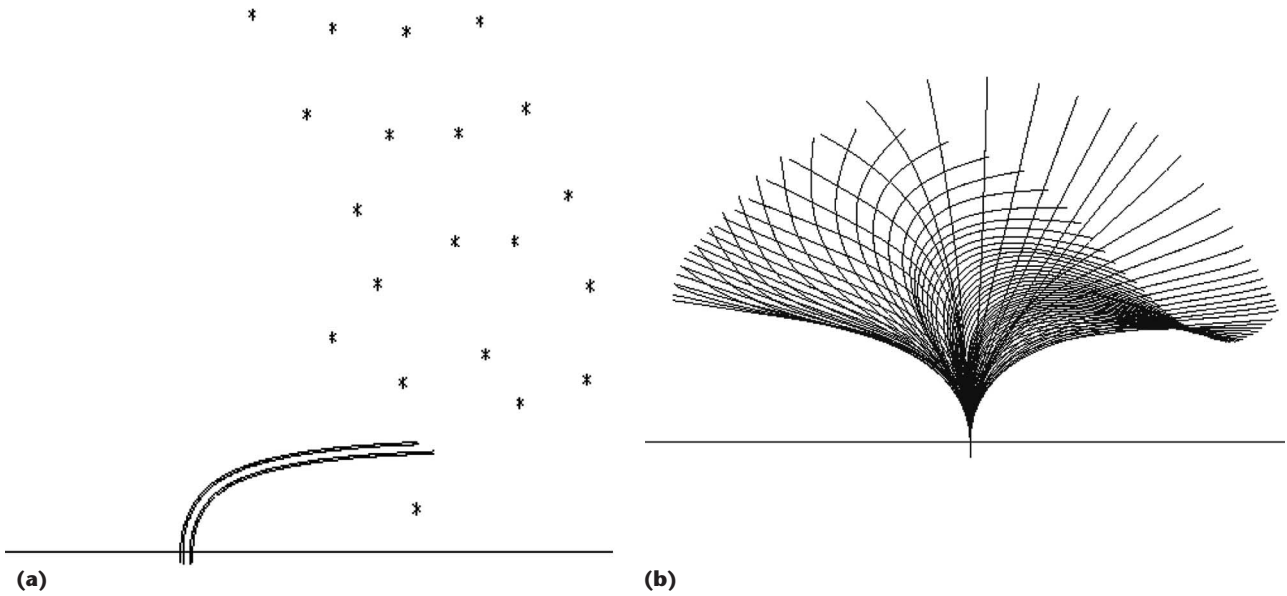
Figure 6. Cilium. (a) A two-microtubule cilium nearing the end of its power stroke. Asterisks denote fluid markers, which we initially placed initially directly above the base of the cilium in a rectangular array. The displacement to the right is the result of the net fluid flow induced by the beating cilium. (b) A ciliary waveform showing a single filament at equally spaced time intervals.
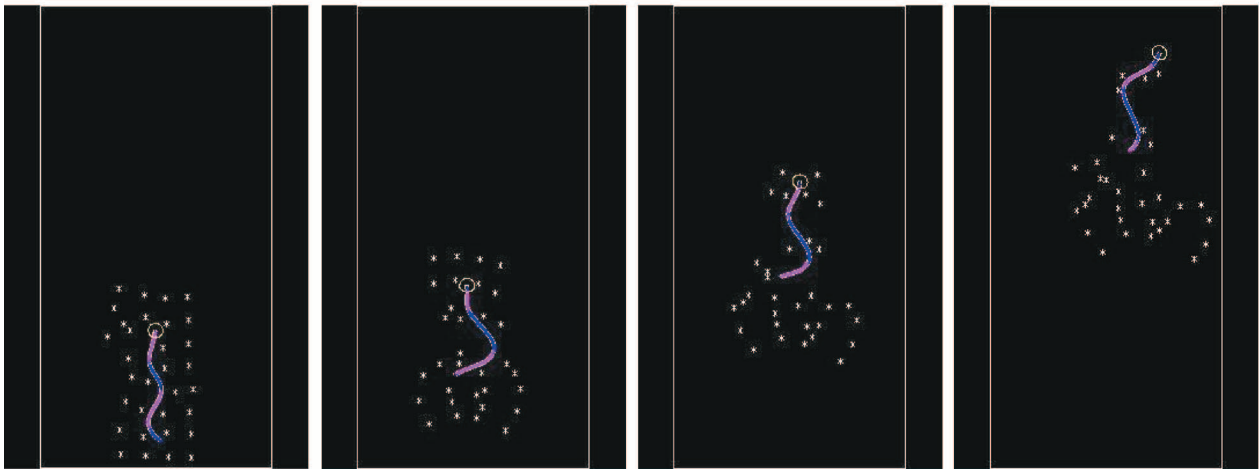
Figure 7. A sequence of a two-microtubule sperm cell swimming upwards as a wave passes from base to tip. The red (blue) color indicates that the right (left) family of dyneins is activated at that position of the flagellum. Asterisks denote fluid markers.

trol model. The beating cilium does indeed result in a net displacement of fluid in the direction of the power stroke, and the sperm cell does indeed swim in the direction opposite that of the wave. We have shown elsewhere[12] that making different assumptions about the internal dynein activation mechanisms does results in different swimming behavior. In particular, when we altered the curvature control model to change the effective time scale of dynein kinetics, the time of a single beat changes significantly, along with

the entire waveform of the flagellum.

Computational fluid dynamics along with biological modeling provides a powerful means for studying the internal force-generation mechanisms of a swimming organism. The integrative approach presented here lets us use computer simulations to examine theories of physiological

processes such as dynein activation in a beating cilium and muscle dynamics in invertebrates. The success of these models depends both on the continued development of robust and accurate numerical methods, and the interdisciplinary collaboration of computational scientists and biologists. We expect that this work will have an impact on understanding biomedical systems such as sperm motility in the reproductive tract and mucus-ciliary transport in both healthy and diseased respiratory tracts, as well as the complex coupling of electrophysiology, muscle mechanics, and fluid dynamics in aquatic animal locomotion. ⊂§

References

1. C.S. Peskin, "The Immersed Boundary Method," *Acta Numerica*, vol. 11, 2002, pp. 479–517.

2. S. Childress, *Mechanics of Swimming and Flying*, Cambridge Univ. Press, 1981.

3. J.L. Lighthill, Mathematical Biofluiddynamics, SIAM Press, 1975.

4. R. Cortez, "The Method of Regularized Stokeslets," *SIAM J. Scientific Computing*, vol. 23, no. 4, 2001, pp. 1204–1225.

5. J. Gray and H.W. Lissmann, "The Locomotion of Nematodes," *J. Exploratory Biology*, vol. 41, 1964, pp. 135–154.

6. C.E. Jordan, "Scale Effects in the Kinematics and Dynamics of Swimming Leeches," *Canadian J. Zoology*, vol. 76, 1998, pp. 1869–1877.

7. M. Murase, *The Dynamics of Cellular Motility*, John Wiley & Sons, 1992.

8. G.B. Witman, "Introduction to Cilia and Flagella," *Ciliary and Flagellar Membranes*, R.A. Bloodgood, ed., Plenum, 1990, pp. 1–30.

9. J. Gray and G. Hancock, "The Propulsion of Sea-Urchin Spermatozoa," *J. Exploratory Biology*, vol. 32, 1955, pp. 802–814.

10. S. Gueron and K. Levit-Gurevich, "Computation of the Internal Forces in Cilia: Application to Ciliary Motion, the Effects of Viscosity, and Cilia Interactions," *Biophyscial J.*, vol. 74, 1998, pp. 1658–1676.

11. R. Dillon and L.J. Fauci, "An Integrative Model of Internal Axoneme Mechanics and External Fluid Dynamics in Ciliary Beating," *J. Theoretical Biology*, vol. 207, 2000, pp. 415–430.

12. R. Dillon, L.J. Fauci, and C. Omoto, "Mathematical Modeling of Axoneme Mechanics and Fluid Dynamics in Ciliary and Sperm Motility," *Dynamics of Continuous, Discrete and Impulsive Systems*, vol. 10, no. 5, 2003, pp. 745–757.

Ricardo Cortez is an associate professor of mathematics at Tulane University and associate director of the Center for Computational Science at Tulane and Xavier Universities. His research interests include numerical analysis, scientific computing, and mathematical biology. He has a PhD in applied mathematics from the University of California, Berkeley. Contact him at rcortez@tulane.edu.

Nathaniel Cowen is a PhD candidate in mathematics at the Courant Institute of Mathematical Sciences. His research interests include computational biofluid dynamics, which involves mathematical modeling of biological systems (including both swimming organisms and internal physiological flows), computational fluid dynamics, and parallel computing. He is a member of the Society for Industrial and Applied Mathematics. Contact him at cowen@cims.nyu.edu.

Robert Dillon is an associate professor of mathematics at Washington State University. His research interests include mathematical modeling of tumor growth, limb development, and flagellar and ciliary motility. He has a PhD in mathematics from the University of Utah. He is a member of the Society for Mathematical Biology, the Society for Industrial and Applied Mathematics, and the American Mathematical Society. Contact him at dillon@math.wsu.edu.

Lisa Fauci is a professor of mathematics at Tulane University and an associate director of the Center for Computational Science at Tulane and Xavier Universities. Her research interests include scientific computing and mathematical biology. She has a PhD in mathematics from the Courant Institute of Mathematical Sciences in 1986. She is member of the Council of the Society for Industrial and Applied Mathematics. Contact her at fauci@tulane.edu .